Fatigue life prediction of stents in a realistic coronary stenosis model

***Xinyang Cui[1], Qingshuai Ren[1,2], †Aike Qiao[1], Gaoyang Li[1], Zihao Li[1]**

[1]College of Life Science and Bioengineering, Beijing University of Technology, Beijing, CHINA

[2] Institute of Mechanics, Chinese Academy of Science, Beijing, CHINA

*Presenting author: xinyangcui@qq.com

†Corresponding author: qak@bjut.edu.cn

Abstract

Background The clinical outcome and fatigue life of stent are closely related to the biomechanical environment of coronary stenosis. In order to predict fatigue life of coronary stents, the stents' adaptability and safety in a realistic stenosis model combined with the clinical data was studied in this paper.

Methods Coronary artery stenosis models were built with Mimics based on CT angiography (CTA) data. Finite element method (FEM) was used to simulate the stent expansion in a realistic and an idealized coronary stenosis model. The stress/strain of the two different models was compared. Based on the mechanical analysis, the influence of cyclic loading effect on the fatigue life of the stents was studied. Stents' fatigue rupture was calculated with Goodman diagram, and the fatigue performance parameters such as the cycle to failure, the fatigue life, fatigue safety factor (FSF), cumulative fatigue damage rate were also analyzed.

Results The maximum stresses in the stent, plaque, and the vessel wall in the realistic stenosis model were 413.8 MPa, 6.06 MPa, and 3.39 MPa, respectively. While in the idealized model, they were 418.3 MPa, 4.46 MPa, and 1.13 MPa, respectively. Although the maximum stress was always located at the bending area of crowns, the stress distributions were different largely in the two models. The relative error ratios of the maximum stress in the plaque and vessel wall between the two models were 26.4%, 66.7%. In the fatigue analysis, the stent would not fail for fatigue rupture calculated by Goodman diagram. The closest point to the fatigue limit was also located at the inner bend of crowns. The predicted number of cycles to failure was $5.32*10^8$, the fatigue life was 14 years, the FSF was 2.8, and the maximum cumulative fatigue damage rate was about 71.5%.

Conclusion The mechanical parameters (stress/strain) were associated with the realistic coronary stenosis model. It is feasible to use a realistic model to calculate the accurate stress/strain for a coronary stent to predict the dangerous point and to evaluate the accurate fatigue performance parameters. This method can serve as a useful tool to support interventional planning for stent implantation in order to minimize the risk of fatigue fracture.

Keywords: Endovascular stent, Stenosis, Biomechanics, Fatigue life prediction.

1. Introduction

In the last decades, stent intervention has become common in clinical to treat cardiovascular disease [1]. Currently, 85% of coronary interventions involve stents [2], adding up to more than 1 million stents per year [3]. But stent failure and fracture (SF) is an inherent risk of stenting [4], and coronary stent fracture (CSF) rate occurred in up to 30% [5,6]. Fractured stents lose their ability to scaffold occluded arteries and may cause restenosis [7], thrombosis [8], or artery perforation [9].

Stent failure can be caused by the mechanical loading, either monotonic or cyclic loading during deployment or service, respectively. Cyclic loading is due to the pulsatile blood pressure or due to vessel movements imposing bending, torsion, or tension/compression on the stent [10]. In the following, we will refer to the failure due to cyclic loading as fatigue. The computer-based design modeling represents an assessment tool for the prediction of stent performance and fatigue life [11, 12].

Computational models have been widely used for their ability to replicate the biomechanical response of medical devices under physiological conditions [14]. From the viewpoint of mechanical, the complex biomechanical environment caused by plaques may lead to CSF [13].

Researchers usually simulate the stent expansion process using idealized models [14,15,16], while many researchers have also used realistic models with the angiography and vascular ultrasound technology in recent years [17]. But the contrast of mechanical parameters (stress/strain) in the two models needs further research.

A study used a patient's arterial geometry data to evaluate the fatigue performance of peripheral stents [18]. But there was few research on the fatigue parameter based on the expansion of stents in a realistic coronary model. [19, 20], which provides new insights into the coronary stent design and failure mechanism.

In this study, structural finite element models were implemented to simulate the stent expansion in a realistic stenosis coronary artery model with the angiography and vascular ultrasound technology. The stresses and strains in the stent, plaque and vessel wall in an idealized model and a realistic model were compared to quantify the response with the presence of a realistic geometrical plaque. To investigate the effects of cyclic blood pressure on the fatigue resistance of the stent, not only Goodman diagram but also the fatigue performance parameters such as the cycle to failure, the fatigue life, fatigue safety factor (FSF), cumulative fatigue damage rate were analyzed.

The information may be helpful in predicting the stent strut fracture and assessing the fatigue life for a coronary stent. This study may eventually help designers to optimize the stent geometry structure, for physicians in their diagnosis and intervention surgical decision

making process.

2. Methods

2.1 3D model reconstructed

Coronary angiography was used to detect coronary atherosclerosis for a 56-year-old male patient. Left coronary artery (LCA) lesion (Fig. 1a) was detected. The realistic stenosis vascular model was reconstructed based on the clinical data of blood vessel and plaque. Firstly, the CT angiography (CTA) data at end-diastole was selected and digitized by using the medical image processing software Mimics 15.0 to eliminate the respiratory and cardiac motion artifacts. Then the coronary arterial tree was reconstructed, as shown in Fig. 1b. Figure 1c shows the narrow segment of blood vessel, which was obtained from the coronary arterial tree with red marker.

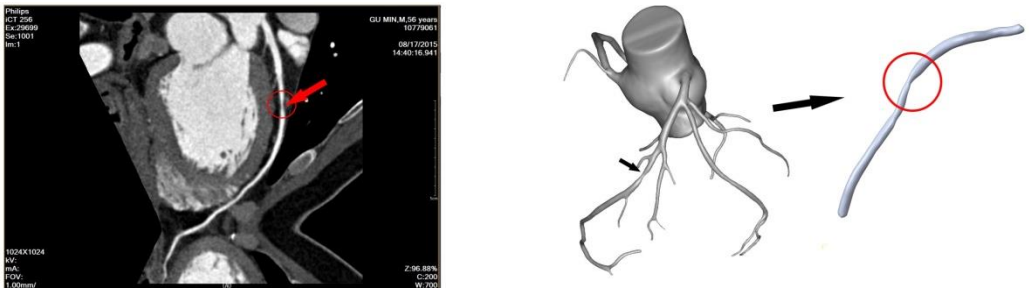

a b c

Figure 1. 3D model reconstruction of coronary stenosis

The stenosis segment was repaired by using the software “Freeform Modeling Plus” based on the data of coronary physiological parameters. A realistic healthy blood flow model was established, as shown in Fig. 2a. The realistic plaque geometry was obtained from the logic subtraction between the healthy and stenotic vessel. Besides, the realistic plaque model was reconstructed combined with its geometry data by “Solid Works 15.0”. The healthy vessel model was obtained by offsetting the healthy blood flow from the physical parameters of the coronary artery wall. Eventually, the realistic plaque model was implanted into the healthy blood vessel to establish the realistic coronary stenosis model, which was shown in Fig. 2b. Figure 2c shows the geometry size of the realistic atherosclerotic lesions of blood vessels. The internal diameter of the blood vessel was 1.62 mm, the length of the stenosis (i.e., the length of the plaque) was 4.62 mm, and its diameter was 0.87 mm.

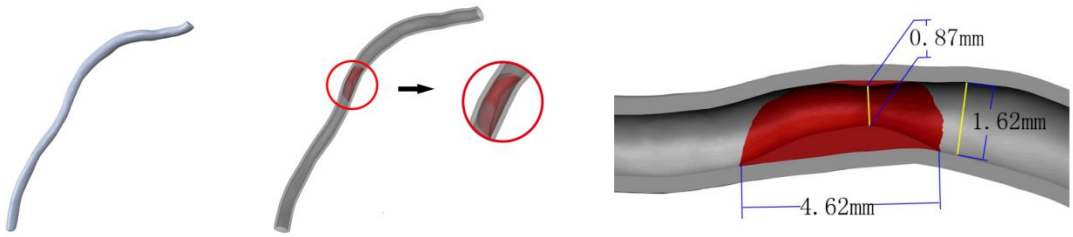

a b c

Figure 2. Reconstruction of vessel wall and plaque

2.2 Parametrized stent design

In order to design a new stent, the size of the narrow blood vessels was taken into consideration to ensure the implementation of the percutaneous coronary artery. The 3D geometry of the repeatable units of the stent was generated by using Pro/Engineer. The single unit cell consisted of 12 crowns with square shaped struts formed a circular stent (diameter=0.6 mm) as shown in Fig.3. The 6 unit cells were linked by I – link bars, and the parameters of the designed stent were shown in Fig. 3, too.

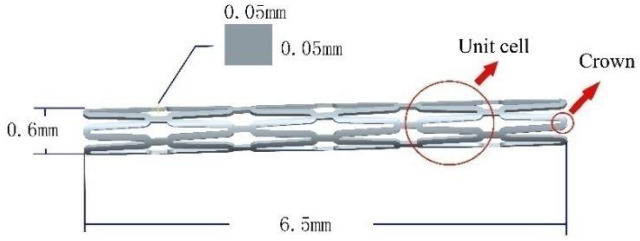

Figure 3. Geometrical model of the stent with I-link

2.3 Meshed models and material models

In this part, the vessel wall, plaque and the stent were meshed with the aid of the software Hypermesh11.0 respectively. Both the realistic vessel wall and corresponding plaque model (as shown in Fig. 4a) were meshed with tetrahedron element, which was relatively denser and would avoid the disturbance of the irregular structures in a realistic stenosis model. Since the realistic model and the stent were deformed largely in the expansion process, the stent was meshed with the linear tetrahedron element to prevent deformity interference deformation, as shown in Fig. 4b. The stent was positioned inside the stenosis coronary artery, and the combined model was meshed shown in Fig. 4c. The detail information of the meshes was shown in Tab. 1.

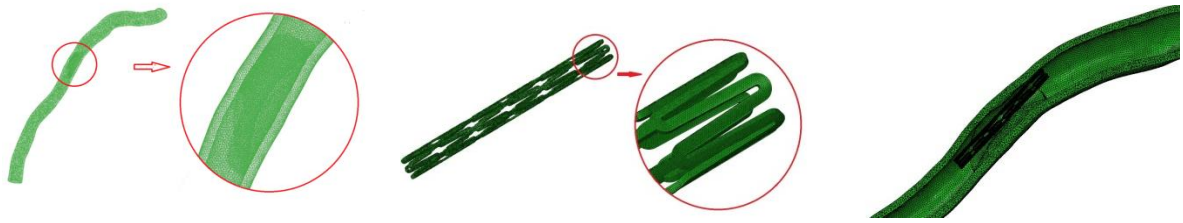

a b c

Figure 4. Mesh of the realistic model.

Table 1. Mesh information and material properties of the stent and vessel model

Models	Element types	Number of elements	Number of nodes	Material properties	Young's modulus (GPa)	Poisson ratio	Yield strength (MPa)
Stent	C3D4	674 335	175 809	304 Stainless steel(304SS)	193.00000	0.270	207
Plaque	C3D4	37286	9366	Calcified Coronary Atherosclerotic Plaque	0.00219	0.499	—
Vessel wall	C3D4	543 974	124930	Calcified vascular cell	0.00175	0.499	—

The material of the vessel wall and the corresponding calcified plaque were ideally linear

elastic, isotropic and incompressible, while the material of the stent was bilinear elastic-plastic. The detailed information of the combination was shown in Tab. 1, too.

2.4 Boundary conditions

Finite Element Method (FEM) was applied to simulate the deployment of a 304 Stainless steel (304SS) stent expanding in the coronary artery and the subsequent deformation under diastolic-systolic cyclic loading conditions. The commercial FEM tool ABAQUS/Standard 6.13 was used to run the simulations.

The stent was positioned inside the coronary artery (Fig. 4c). Then uniform radial deformation load was imposed on the stent's inner surface along the vertical axis to simulate the expansion process. Furthermore, nodes belonging to the stent surface were constrained in the tangential direction to avoid any rotation inside the vessel. The artery was constrained in the section near the plaque to prevent any displacements and rotations. To mimic possible interactions between the stent and the plaque, the sliding friction contact surfaces were introduced with the friction factor being 0.2 [21], with the same value for the interaction ratio between the stent and the vessel wall. Plaque and the vessel inner surfaces were assumed to be bonded, in order to ensure the models' displacement.

The simulated loading steps were as follows:

The first step: stent expansion. After percutaneous transluminal angioplasty (PTA), the balloon inflation was modeled through a displacement-driven analysis, where a uniform radial deformation was imposed to inner stent surface, till the diameter is equal to 1.1 times of the vessel inner diameter. This value was chosen to ensure the achievement of a residual stenosis lower than 30% that is required by clinicians for continuing with the stenting procedure [22]. At the end of this step, the deformation was deflated, and the plaque and artery vessel wall were elastically recoiled.

The second step: diastolic-systolic cyclic loading. After expanding in the stenosis coronary artery, the stent undergoes pulsatile loading that arisen from oscillation of the internal blood pressure. This phenomenon was modeled by applying the loading boundary conditions illustrated in Fig. 5. In particular, the internal blood pressure oscillated between 80 mmHg and 120 mmHg from diastole to systole and was applied to the inner surfaces of the stent. Diastolic heart filling and systolic contraction steps were simulated for three cardiac cycles (Fig. 5). It was believed that the constitutive model response get stabilized after three loading cycles [22]. The pressures of the three loading cycles were performed to simulate the effect on the material model by using ABAQUS. These cardiac cycles simulation were conducted to determine the alternating maximum strain induced in the stent as a result of these cyclic loading patterns, and the pressure loading was based on Food and Drug Administration (FDA) test requirements [23]. It was also recommended by the FDA that Goodman fatigue life analysis be used to determine the FSF subjected to physiologic loading up to $4*10^8$ fatigue cycles.

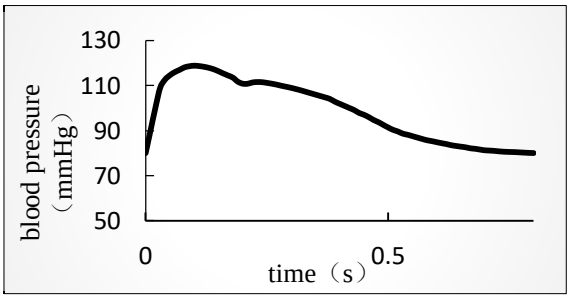

Figure 5. The blood pressure wave form in a cardiac cycle

2.5 Establishment of an idealized model as the control group

A 3D model for the stenosis coronary artery with the idealized structure was established, and the same plaque and vessel material properties were defined in the realistic model, as shown in Fig. 6. The geometry of idealized model is obviously uniform and symmetric, and other information and boundary conditions are the same in the realistic coronary model. The mechanical properties in the different models were compared, and the effect of realistic geometry of a plaque on the stent mechanical behavior was explored.

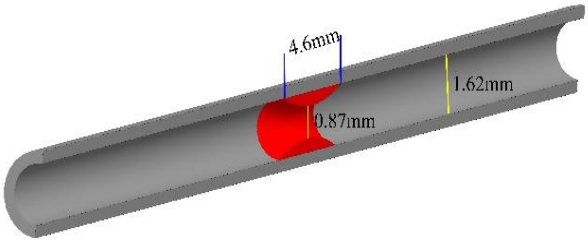

Figure 6. The geometry of the idealized model

3. Results

3.1 Analyses of mechanical properties (stress/strain)

At the end of stent expansion, the deformation loading was deflated. The plaque and artery vessel wall were elastically recoiled, and consequently the stent protrusion moved towards the center of the lumen. The presence of plaque generated a greater resistance to the vessel. In order to compare the effect of two different models on the mechanical properties, the stress distributions of the stent, plaque and inner vessel wall were shown in Fig. 7 and Fig. 8, respectively. The stress distribution of idealized model was symmetric (Fig. 8). However, the results of the realistic model were completely different (Fig. 7).

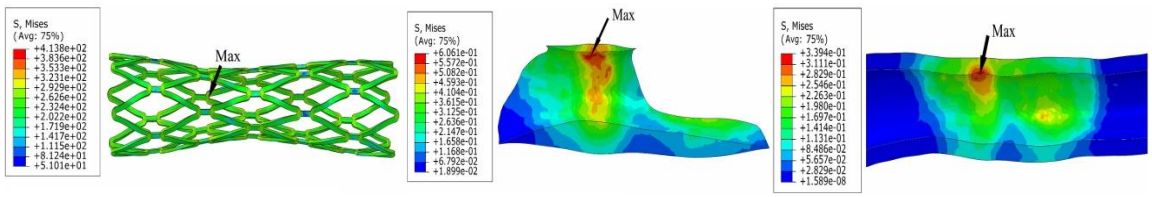

a b c

Figure 7. The stress distribution of complete expansion stage in a realistic model

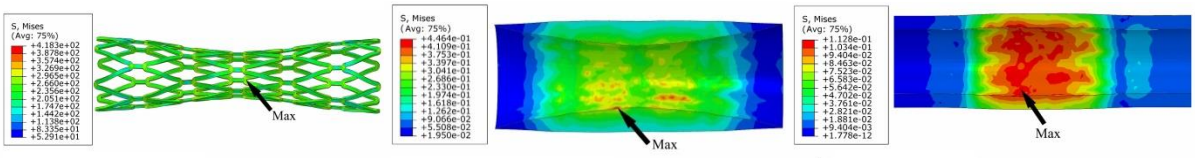

a b c

Figure 8. The stress distribution of complete expansion stage in an idealized model

In Fig.7a, the higher stress region was observed in the stent struts close to the calcified plaque, and the maximum stress was 413.8 MPa localized in the bend of the crown, where the dangerous position in the stent structure must be located. The minimal stressed regions were located in the middle position of the bridging I-links. While in the idealized model, the maximum stress of the stent was 418.3 MPa (Fig. 8a). Comparing Fig. 7a with Fig. 8a, the position of the maximum stress changed, but was still located in the bend of the crown.

The higher stress region of plaque was located in the stenosis, and there was a correlation between the stress distribution and the shape of the plaque. The stress distributed uniformly along the axis in the idealized model (Fig. 8b), and was different from the stress distribution in the realistic model (Fig. 7b). Quantitatively, the maximum stress in the plaque was 6.06 MPa in the realistic model (Fig. 7b), while that in the idealized model was 4.46 MPa (Fig. 8b). The relative error ratio was about 35.9%. This revealed that the realistic geometric parameters greatly influenced the result of the mechanics.

From the Fig. 7c and the Fig.8c, the difference of stress distribution in the inner vessel wall between the realistic model and idealized model was obvious. In the higher stress area, the stress was mainly 1.13 MPa~3.39 MPa (Fig. 7c), while in the realistic model it was mainly 0.56 MPa~1.13 MPa (Fig. 8c). The maximum stress on the inner vessel wall of the realistic model was 3.39 MPa, while in the idealized model it was 1.13 MPa. The relative error ratio was about 200.9%.

We supposed that a realistic coronary model can provide accurate stress/strain calculations. It is evident that the highest stresses are observed near the connectors between the stent struts (in agreement with the Ref. [17]). In addition, higher stresses were observed in the stent struts close to the calcified plaque region (in agreement with the Ref. [20]). The coronary stenosis model including a realistic plaque can serve as a useful tool for physicians in their diagnosis and intervention surgical decision making process. Therefore, the data we used in the following fatigue analysis were calculated by the realistic model.

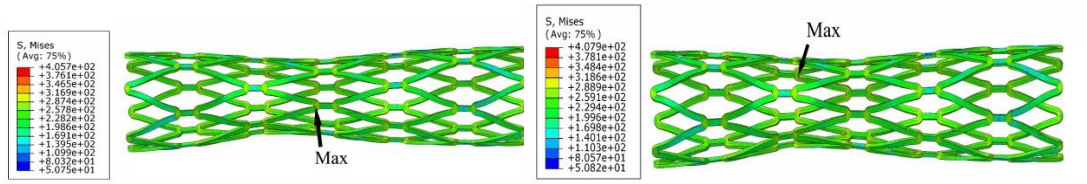

a b

Figure 9. The stress distribution in the stent under different pressures

Figure 9 shows the stress distribution under the systolic and diastolic blood pressure using a realistic model. When the systolic pressure was 120 mmHg, the maximum stress was 405.7 MPa, as shown in Fig. 9a. When the diastolic pressure was 80 mmHg, the position of the maximum stress changed, and the maximum stress changed. The maximum stress was 407.9 MPa, as shown in Fig. 9b. The numerical fluctuation of the stress was not obviously compared with the stress during the stent expansion process. It can be seen from the Fig. 9a and Fig. 9b that stress distribution has the same trend under different pressures, and the maximum stress located in the inner bend of crowns, while the minimal stress located in the I-link. In order to analyze the influence of cyclic loading effect, we calculated the fatigue parameters of the stents.

3.2 Fatigue life analysis

Stress values obtained after the second cycle were equal to those obtained after the third cycle; hence, a Goodman life analysis was performed using the oscillating multi-axial stress state obtained during the second cardiac cycle [13].

3.2.1 Goodman diagram for failure prediction

The FDA recommends that the fatigue resistance of the stent to physiologic loading should be determined using Goodman analysis. Due to the lack of exact information on the mechanical behavior of the material used to fabricate the stent, the literature data were used to draw the stent material fatigue limit on the Goodman diagram [24]. In particular, the endurance limit for zero mean stress was assumed to be equal to 186 MPa while ultimate stress was equal to 520 MPa.

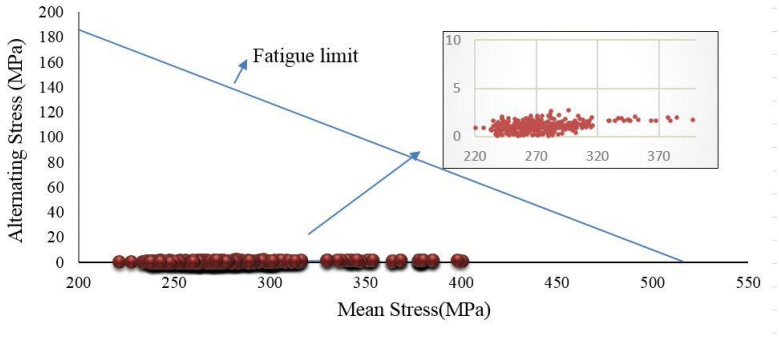

Figure 10. Goodman diagram for the fatigue analysis of stent

The mean stress and alternating stress could be calculated with the stress state of dilation recoil and external loading phase, then all the calculating results on the coordinate figure could be plotted to obtain the Goodman diagram (Fig. 10). As shown in Fig. 10, the x-axis represented the mean stress and the y-axis represents the alternating stress. The slanting line in Fig. 10 was the fatigue limit line (Goodman line), and the intersection point between the fatigue limit and the x-axis was the ultra-tensile strength of 304SS material. The intersection point between the fatigue limit and the y-axis indicated the fatigue endurance strength of the 304SS material. In theory, the closer it was to the fatigue limit, the more dangerous to the structure. As shown in Fig. 10, all the points fallen below the limit line of the material and the stent was able to pass the fatigue life of $4*10^8$ cycles under pulsatile fatigue loading. The stent would not fail with fatigue rupture.

3.2.2 Stent Service Life Prediction

Goodman fatigue life analysis has been widely used for assessing the device fatigue resistance and providing an indication of device chronic durability. The results showing the most dangerous points (Fig. 11) were located in the bend of the crowns, and the data of the most dangerous points were shown in the Tab. 2. This finding is in agreement with the Ref. [16], which means that the maximum strain occurred at the inner surface of the crowns.

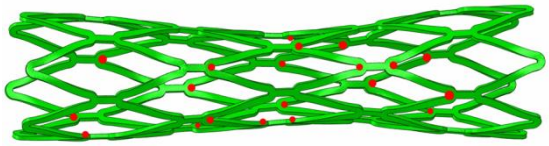

Figure 11. The most dangerous points (red marks) in the stent fatigue prediction

According to the cumulative fatigue damage rate descending order, the predicted cycles to failure of the most dangerous point was $5.32*10^8$ (14 years equivalent), FSF>1, and the cumulative fatigue damage rate was 71.45%. The FDA requires the fatigue testing should include in vitro testing at least $4*10^8$ cycles (10 years equivalent), which indicates the stent is safe in theory.

In this study, the FSF of the most dangerous point was 2.8>1. Compared with the results in Ref. [16] (where FSF=2.06), the stent structure used in this paper was relatively safer. The FSF is defined as the ratio of the strain amplitude against the modified endurance limit, and FSF of less than 1.0 indicates the stent fatigue failure. As shown in the Tab.2, the trend of FSF is similar to that of the fatigue cycle, while the fatigue cycle quantified the proximity of the mean strain and strain amplitude at the given integration points to the Goodman failure line.

In Tab.2, the cumulative fatigue damage rate of the most dangerous point was 71.45%. The referenced methods for calculating cumulative fatigue damage rate (Ref. [24] and Ref. [25]) were quantitative standard for evaluating the fracture rupture. The calculating cumulative fatigue increases with applied load cycles in a cumulative manner, and the stent structure would fracture when the cumulative fatigue damage rate reached 100%. As shown in the Tab. 2, the cumulative fatigue damage rate was all below the 71.45%, and hence the stent structure is safe.

Table 2. The fatigue performance parameters of the most dangerous points

Number	Predicted number of cycles to failure	Fatigue life (a)	FSF	Cumulative fatigue damage rate (%)
1	5.32E+08	14	2.8	71.45
2	5.41E+08	14.25	2.81	70.18
3	5.56E+08	14.63	2.81	68.33

4	7.00E+08	18.42	2.84	54.29
5	7.43E+08	19.55	2.86	51.16
6	7.78E+08	20.47	2.86	48.86
7	8.20E+08	21.58	2.85	46.34
8	8.77E+08	23.07	2.86	43.34
9	8.87E+08	23.34	2.86	42.85
10	8.91E+08	23.44	2.89	42.66
11	9.38E+08	24.7	2.86	40.49
12	9.71E+08	25.56	2.88	39.12
13	1.19E+09	31.27	2.92	31.98
14	1.22E+09	32.15	2.9	31.11
15	1.24E+09	32.64	2.92	30.64
16	1.25E+09	32.97	2.93	30.33
17	1.26E+09	33.17	2.95	30.15
18	1.27E+09	33.4	2.95	29.94
19	1.33E+09	35.04	2.94	28.54
20	1.34E+09	35.39	2.99	28.25

According to the stress analysis and fatigue analysis, we can deduce that maximum stress was always located at the bend of crowns in all simulation procedures, the closest point to the fatigue limit was also located at the inner bend of crowns of stent, and the fatigue analysis results confirmed the mechanical analysis again.

4. Discussion

Numerical models are nowadays a widely recognized useful tool to study the interaction of the stent with tissues and organs [26]. Stent fracture caused by cyclic loading is becoming a key issue in interventional treatment [1]. Clinical studies showed that factors such as stent design, vascular district properties and loading conditions are possible causes of stent fracture. In this study, the interaction of stents, the plaque and the vessel wall in a realistic model and an idealized model were simulated, and the importance of the plaque geometry in the mechanical analysis was confirmed. The finite element method to simulate the effects of cyclic loading experienced by a stented artery during a cardiac cycle was presented. The evaluation was based on the numerical results to build the Goodman Diagram. In the fatigue life prediction, the FSF quantified the proximity of the mean stress and stress amplitude at the given integration points to the Goodman failure line. Cumulative fatigue damage rate analysis played a key role in life prediction of components and structures subjected to field load histories. This method provided an accurate way to predict the stent fatigue life.

This study can surely be improved as from the presence of some limitations. From a modeling point of view, the absence of the balloon has an influence during the inflating process, and the influence of residual stress in the process of crimping was ignored. Future research will be devoted to removing this assumption to have a more realistic description of the stent deployment process. In the fatigue analysis, the stent in the stenosis coronary artery undergoes pulsatile loading conditions that arise from two different phenomena: oscillation of the

internal blood pressure and cardiac wall movement [13], but in this paper we only take the blood pressure into consideration, the next step should focus on the bending fatigue caused by cardiac wall movement. In this paper, material data cited as the strain-based Goodman fatigue life analysis were from several references [24], we should do the material test to get the material data, in order to get more accurate results.

5. Conclusions

The CSF was affected by the complex biomechanical environment caused by the plaques. The mechanical stress/strain was calculated more accurately using a realistic coronary stenosis model. Our results indicated that the maximum stress at all stages was always located at the inner bend of the crowns and the maximum alternating stress was also distributed at the same position, which indicated that the dangerous points were located at the curvature area of the crowns. The effects of cyclic loading on the identification of mechanisms governing stent fatigue rupture were investigated. A better understanding of the failure cycle, the fatigue life, FSF, and cumulative fatigue damage rate may lead to better assessment for the stent fatigue life. This study provided an approach to select and position a stent in order to minimize the risk of fatigue fracture. In fact, this is a general approach and is not limited to 304 stainless steel, and further applications could focus on other metallic materials.

Acknowledgement

The research was supported by National Natural Science Foundation of China (81171107).

References

[1]. Dordoni E, Meoli A, Wu W, et al. (2014) Fatigue behaviour of Nitinol peripheral stents: The role of plaque shape studied with computational structural analyses. *Medical Engineering & Physics* **36**, 842-9.

[2]. Garg S, Serruys PW. (2010) Coronary Stents: Current Status. *Journal of the American College of Cardiology* **56**, S1-S42.

[3]. Li J, Luo Q, Xie Z, et al. (2010) Fatigue life analysis and experimental verification of coronary stent. *Heart & Vessels* **25,** 333-337.

[4]. Satjit A, Mujeeb S, Jason WU, et al. (2010) Stent Fracture in the Coronary and Peripheral Arteries. *Journal of Interventional Cardiology* **23**, 411-419.

[5]. Lim HB, Hur G, Kim SY, et al. (2008) Coronary stent fracture: detection with 64-section multidetector CT angiography in patients and in vitro. *Radiology* **249**, 810-9.

[6]. Nakazawa G, Finn AV, Vorpahl M, et al. (2009) Incidence and Predictors of Drug-Eluting Stent Fracture in Human Coronary Artery. *A Pathologic Analysis. Journal of the American College of Cardiology* **54**:1924-31.

[7]. Scheinert D, Scheinert S, Sax J, et al. (2005) Prevalence and clinical impact of stent fractures after femoropopliteal stenting. J Am CollCardiol. *Journal of the American College of Cardiology* **45**.

[8]. Bessias N, Sfyroeras G, Moulakakis KG, et al. (2005) Renal artery thrombosis caused by stent fracture in a single kidney patient. *Journal of Endovascular Therapy* **12,**516-520.

[9]. Lewitton S, Babaev A. (2008) Superficial Femoral Artery Stent Fracture that Led to Perforation, Hematoma and Deep Venous Thrombosis. *Journal of Invasive Cardiology* **20,** 479-81.

[10]. Auricchio F, Constantinescu A, Conti M, et al. (2015) Fatigue of Metallic Stents: From Clinical Evidence to Computational Analysis. *Annals of Biomedical Engineering*, 1-15.

[11]. Dordoni E, Petrini L, Wu W, et al. (2015) Computational Modeling to Predict Fatigue Behavior of NiTi Stents: What Do We Need? *Journal of Functional Biomaterials* **6**, 299-317.

[12]. James BA, Sire RA. (2010) Fatigue-life assessment and validation techniques for metallic vascular implants. *Biomaterials* **31**, 181-186.

[13]. Morlacchi S, Pennati G, Petrini L, et al. (2014) Influence of plaque calcifications on coronary stent fracture: A numerical fatigue life analysis including cardiac wall movement. *Geological Magazine* **47**, 899-907.

[14]. Ragkousis GE, Curzen N, Bressloff NW. (2014) Simulation of longitudinal stent deformation in a patient-specific coronary artery. *Medical Engineering & Physics* **36**, 467-476.

[15]. Hsiao HM, Chiu YH, Lee KH, et al. (2012) Computational modeling of effects of intravascular stent design on key mechanical and hemodynamic behavior. *Computer-Aided Design* **44**, 757-765.
[16]. Hsiao HM, Wu LW, Yin MT, et al. (2014) Quintupling fatigue resistance of intravascular stents via a simple design concept. *Computational Materials Science* **86**, 57-63.
[17]. Gijsen FJ, Migliavacca F, Schievano S, et al. (2008) Simulation of stent deployment in a realistic human coronary artery. *Biomedical Engineering Online* **7**, 23-23.
[18]. Petrini L, Trotta A, Dordoni E, et al. (2015) A Computational Approach for the Prediction of Fatigue Behaviour in Peripheral Stents: Application to a Clinical Case. *Annals of Biomedical Engineering*, 1-12.
[19]. Marrey RV, Burgermeister R, Grishaber RB, et al. (2006) Fatigue and life prediction for cobalt-chromium stents: A fracture mechanics analysis. *Biomaterials* **27**, 1988-2000.
[20]. Schievano S, Taylor A M, Capelli C, et al. (2010) Patient specific finite element analysis results in more accurate prediction of stent fractures: Application to percutaneous pulmonary valve implantation. *Journal of Biomechanics* **43**, 687-693.
[21]. Yang Z, Zhang HP, Marder M. (2008) Dynamics of static friction between steel and silicon. *Proceedings of the National Academy of Sciences of the United States of America* **105**, 13264-8.
[22]. Dordoni E, Meoli A, Wu W, et al. (2014) Fatigue behaviour of Nitinol peripheral stents: The role of plaque shape studied with computational structural analyses. *Medical Engineering & Physics* **36**, 842-9.
[23]. The guidance for industry and FDA staff: Non-clinical tests and recommended labeling for intravascular stents and associated delivery systems[EB/OL]. Http://www.fda.gov/medicaldevices/deviceregulationandguidance/guidancedocuments/ucm071863.htm,2010-04-18.
[24]. Li HX, Gao YH, Wang XC. (2013) Optimization of stent-balloon system based on surrogate modeling technique. *Journal of Medical Biomechanics*
[25]. Pelton AR, Schroeder V, Mitchell MR, et al. (2008) Fatigue and durability of Nitinol stents. *Journal of the Mechanical Behavior of Biomedical Materials* **1**, 153-64.
[26]. Morlacchi S, Migliavacca F. (2013) Modeling Stented Coronary Arteries: Where We are, Where to Go. *Annals of Biomedical Engineering* **41**, 1428-1444.